

209  
**NASA CONTRACTOR  
REPORT**



**NASA CR-109**

**NASA CR-109**

N64-31205

ACCESSION NUMBER

DATE

NASA CR OR NASA CR AD NUMBER

THRU

CODE

CATEGORY

**REAL-TIME COMPENSATION FOR  
TROPOSPHERIC RADIO REFRACTIVE  
EFFECTS ON RANGE MEASUREMENTS**

*by J. J. Freeman*

Prepared under Contract No. NAS5-1404 by  
J. J. FREEMAN ASSOCIATES, INC.  
Silver Spring, Md.  
*for*

**NATIONAL AERONAUTICS AND SPACE ADMINISTRATION • WASHINGTON, D. C. • OCTOBER 1964**

**REAL-TIME COMPENSATION FOR TROPOSPHERIC RADIO  
REFRACTIVE EFFECTS ON RANGE MEASUREMENTS**

**By J. J. Freeman**

Distribution of this report is provided in the interest of information exchange. Responsibility for the contents resides in the author or organization that prepared it.

Prepared under Contract No. NAS5-1404 by  
J. J. FREEMAN ASSOCIATES, INC.  
Silver Spring, Maryland

for

**NATIONAL AERONAUTICS AND SPACE ADMINISTRATION**

---

For sale by the Office of Technical Services, Department of Commerce,  
Washington, D.C. 20230 -- Price \$0.75

# REAL-TIME COMPENSATION FOR TROPOSPHERIC RADIO REFRACTIVE EFFECTS ON RANGE MEASUREMENTS

by

J. J. Freeman

*J. J. Freeman Associates, Inc.*

## SUMMARY

A formula for the tropospheric contribution to the electro-magnetically measured range is evolved which depends upon the measured value of the surface refractivity and certain average site characteristics. The predictions of this formula were tested against 77 ray-tracings of refractivity profiles measured with radiosondes at thirteen different sites. The rms error in predicted compensation for tropospheric refraction effects on range measurements varied approximately from 1 m at a target elevation angle of 20 mr (milliradians) (approx.  $1^\circ$ ) to 0.03 m at  $90^\circ$ .

31205  
Suther

## CONTENTS

Summary . . . . .	i
List of Symbols . . . . .	iv
INTRODUCTION . . . . .	1
AN APPROXIMATE FORMULA FOR $\Delta R$ . . . . .	2
IMPROVING THE APPROXIMATION . . . . .	3
COMPUTING THE RAY BENDING . . . . .	4
DETERMINATION OF THE PARAMETER $d$ . . . . .	6
THE COMPUTATION PROCEDURE . . . . .	14
PREDICTION RESULTS . . . . .	15
CONCLUSION . . . . .	17
ACKNOWLEDGMENTS . . . . .	17
References . . . . .	17

## List of Symbols

- b bending angle, the angular difference between the tangent to a radio ray at a given point and the ray tangent at the surface
- $b_0$  approximation to  $b$  obtained by integration along the line of sight instead of along the ray path
- c velocity of light in vacuo
- d exponential factor describing the variation of  $N$  with height, reciprocal km
- $G(g) = \sqrt{\pi} g e^{g^2} (1 - \operatorname{erf} g)$
- $g = \sqrt{dr_0/2} \tan \beta_0$
- h height of an arbitrary point above sea level, km
- $h_s$  height of site above sea level, km
- $i_n$  unit principal normal, a unit vector normal to the ray path lying in the osculating plane
- $i_t$  unit vector tangent to the ray path
- K curvature of a path
- $N = (n - 1) \times 10^6 = \text{refractivity}$
- $N_s$  value of  $N$  at the earth's surface
- n radio refractive index
- $R_0$  slant range, km
- $R_e$  electromagnetically determined range, km
- $\Delta R$  contribution to  $R_e$  arising from the refractivity, km
- r distance from the earth's center to an arbitrary point, km
- $r_0$  distance from the earth's center to the earth's surface, km
- s length along a ray path
- TRA tropospheric range adjustment =  $\Delta R$ , km
- $\text{TRA}_{90^\circ}$  TRA for a target whose elevation angle is  $90^\circ$
- $\overline{\text{TRA}}_{90^\circ}$  value of  $\text{TRA}_{90^\circ}$  averaged over many profiles at a given site

$TRA_{90^\circ, p}$  predicted value of  $TRA_{90^\circ}$  obtained from  $TRA_{90^\circ, p} = A + B N_s$ , where A and B are constants for each site

$\alpha$  a variable lying between 0 and 1.

$\beta$  slant range elevation angle at a distance  $r$  from the earth's center

$\beta_0$  slant range elevation angle at the earth's surface; the complement of the angle between the zenith and the slant range at the surface

$\gamma$  elevation angle at a distance  $r$  from the earth's center of the straight line whose elevation angle at the surface is  $\gamma_0$ .

$\gamma_0$  elevation angle of a straight approximation to a radio ray lying between  $\theta_0$  and  $\beta_0$ .

$\epsilon$   $\theta_0 - \beta_0$

$\theta_0$  elevation angle of a radio ray at the earth's surface

$\tau$  time delay of radio wave, seconds

# REAL-TIME COMPENSATION FOR TROPOSPHERIC RADIO REFRACTIVE EFFECTS ON RANGE MEASUREMENTS\*

by

J. J. Freeman

*J. J. Freeman Associates, Inc.*

## INTRODUCTION

The delay incurred by a radio wave between point 0, on the earth's surface, and point 1, above the troposphere, is

$$\tau = \frac{1}{c} \int_0^1 n \, ds .$$

The electromagnetically determined range  $R_e$  between 0 and 1 is

$$R_e = c\tau = \int_0^1 n \, ds ,$$

the integral extending over the curved ray path (Figure 1). Here  $c$  is the velocity of light in vacuo,  $n$  is the index of refraction, and  $s$  signifies length. The true or slant range between 0 and 1 is

$$R_0 = \int_0^1 ds ,$$

the integral being taken along the geometric line joining 0 and 1. The contribution to the measured range arising from the refractivity is

$$\Delta R = \int_0^1 n \, ds - R_0 . \quad (1)$$

\*A condensed version of this paper was presented at the Tropospheric Refractive Effects Meetings, Mitre Corp., Bedford, Mass., November 13-14, 1963, under the title "The Real Time Compensation for Tropospheric Effects on the Measurement of Range and Range Rate," and this earlier version was published in Vol. II of the Proceedings in April 1964.

This paper derives and evaluates a formula which predicts in real time from available ground data the static or slowly varying part of  $\Delta R$  arising from the troposphere, for a target above the troposphere. The problem may be stated more specifically as follows: Surface refractivity  $N_s$ , the apparent or measured target elevation angle  $\theta_0$ , and the apparent or measured range  $R_e$  are given. From these data the adjustment  $\Delta R$ , which is subtracted from  $R_e$  to yield  $R_0$ , is estimated.

## AN APPROXIMATE FORMULA FOR $\Delta R$

The range increment  $\Delta R$  arises from the increase in path length due to both the curvature of the ray path and the decreased wave propagation velocity through the medium. However, it can be shown that the partial contribution (Reference 1) to  $\Delta R$  arising from the increase in path length is of the second order in  $n-1$ , whereas the contribution arising from the decrease in wave velocity is of the first order in  $n-1$ . As a first approximation,

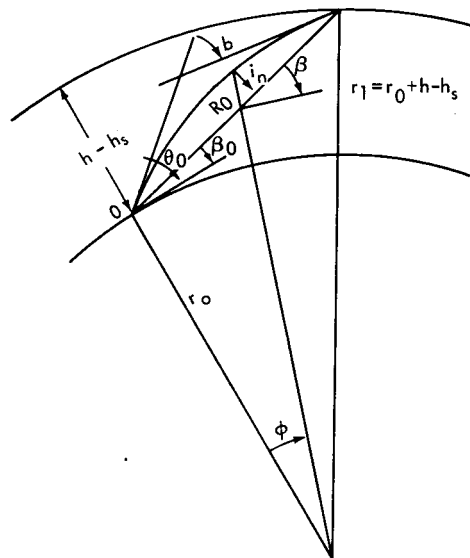


Figure 1—Geometry of the ray path.

$$\Delta R = \int_0^1 (n-1) ds, \quad (2)$$

where the integral is now taken along the slant range path. This mathematical stratagem permits the direct integration of the value of  $\Delta R$  when  $n-1$  has a simple functional dependence on height.

It is reasonable to assume (References 2-4) that the distribution of  $N = (n-1) \times 10^6$  is approximately

$$N = N_s e^{-d(h-h_s)} \quad (3)$$

where  $d$  is a parameter,  $N_s$  is the surface refractivity at a locality which is height  $h_s$  above sea level, and  $h$  designates the altitude of an arbitrary point above sea level. Then Equation 2 may be integrated explicitly to yield (Reference 5)

$$\Delta R = 10^{-6} \int_0^1 N ds = \frac{10^{-6} N_s \sqrt{\pi}}{d \sin \beta_0} \operatorname{erf}^2 g (1 - \operatorname{erf} g), \quad (4)$$

where

$$\operatorname{erf} g = \frac{2}{\sqrt{\pi}} \int_0^g e^{-x^2} dx ,$$

and

$$g = \sqrt{\frac{dr_0}{2}} \tan \beta_0 . \quad (5)$$

Here  $r_0$  is the distance from the earth's center to the surface,  $\beta_0$  is the slant range elevation angle at the ground (Figure 1), and all lengths are expressed in kilometers. For large  $g$  Equation 4 has the asymptotic expansion

$$\Delta R = 10^{-6} \int_0^1 N ds = \frac{10^{-6} N_s}{d \sin \beta_0} \left( 1 - \frac{1}{2g^2} + \frac{1 \times 3}{4g^4} - \frac{1 \times 3 \times 5}{8g^6} + \dots \right) . \quad (6)$$

## IMPROVING THE APPROXIMATION

Although Equation 4 is a fair approximation of the tropospheric range contribution for an exponential atmosphere, it is consistently too high, the excess increasing as the ray elevation angle decreases. The reason\* is that the slant range path of integration on which  $\int N ds$  was computed is always below the true ray path; since  $N$  decreases with height, the values of  $N$  used in the integral are always too large. This results in an upper limit to the true value. On the other hand, integrating  $N ds$  along the straight line having the apparent direction of the target yields too small a value. Accordingly, some line lies between  $\theta_0$  and  $\beta_0$  along which  $\int N ds$  most closely approximates the same integral taken along the ray path (Figure 2); the surface elevation of the line  $\gamma_0$  lies somewhere between  $\theta_0$  and  $\beta_0$ . Or

$$\gamma_0 = \theta_0 - \alpha(\theta_0 - \beta_0) ,$$

where  $\alpha$  is some number, lying between 0 and 1, which will be empirically determined. Since for

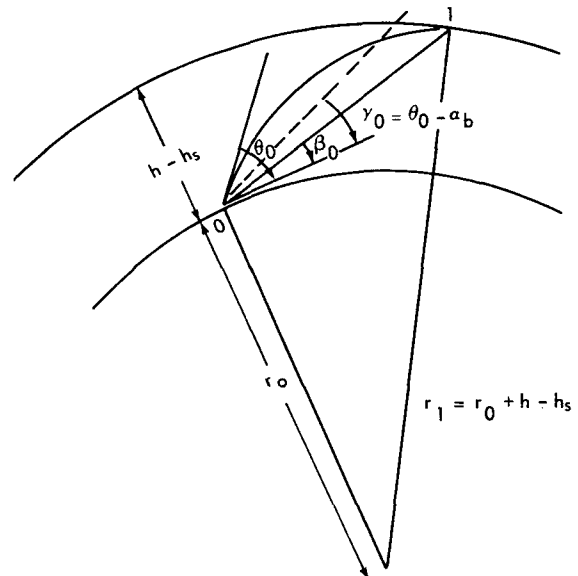


Figure 2—Geometry of the path of integration (dotted line).

\*Mr. G. D. Thayer of the National Bureau of Standards, Boulder, Colorado, pointed this out.

distant targets (above 160 km) the bending angle  $b$  (see Figure 1) approximates  $\theta_0 - \beta_0$ , then  $\gamma_0 = \theta_0 - ab$ . The following section derives an analytic approximation for  $b$ .

## COMPUTING THE RAY BENDING\*

Along a ray path, from Fermat's principle (Reference 7)

$$\frac{d}{ds} = \left( n \frac{dx_i}{ds} \right) = \frac{\partial n}{\partial x_i},$$

where  $i = 1, 2, 3$ . Expressed vectorially,

$$\frac{d}{ds} (ni_t) = \nabla n = n \frac{di_t}{ds} + i_t \frac{dn}{ds},$$

where  $i_t$  is the unit vector tangent to the ray path. But

$$\frac{di_t}{ds} = K i_n,$$

where  $i_n$  is the unit principal normal, and  $K$  is the curvature, i.e., the arc-rate of rotation of the tangent. Since the bending angle  $b$  between two points on the path is defined as the angle the tangent has rotated through in traveling between the two points,

$$\frac{di_t}{ds} = \frac{i_t(s+ds) - i_t(s)}{ds} = \frac{db}{ds} i_n,$$

$$\nabla n = n \frac{db}{ds} i_n + i_t \frac{dn}{ds},$$

Since  $i_t$  and  $i_n$  are normal to each other,

$$\frac{db}{ds} = \frac{1}{n} i_n \cdot \nabla n = i_n \cdot \nabla \ln n.$$

Integration gives

$$b = \int i_n \cdot \nabla \ln n ds.$$

\*See Reference 6.

Since  $n = 1 + N \times 10^{-6}$ , then, to terms of the first order in  $n - 1$ ,

$$b = 10^{-6} \int \mathbf{i}_n \cdot \nabla N ds .$$

From Figure 1, if  $N$  is a function only of  $r$ , the radial distance from the earth's center,

$$b = - \int \frac{dN}{dr} \cos \theta ds ,$$

where  $\theta$  is the complement of the angle between the ray and the radius vector, i.e., the ray elevation at  $r$ ,  $\theta$ .

Since any straight line between the slant range path and the ray path differs only slightly from the latter, the integral will be evaluated along this straight line path, expressed in polar coordinates,

$$r \cos \gamma = r_0 \cos \gamma_0 = \text{constant},$$

where  $\gamma$  is the elevation angle of the path at distance  $r$  from the earth's center. Accordingly, the integral along this path reads

$$b = r_0 \cos \gamma_0 \int \frac{1}{r} \frac{dN}{dr} ds . \quad (7)$$

If it is assumed that  $N$  is given by Equation 3, then Equation 7 becomes

$$b = - r_0 d \cos \gamma_0 \int \frac{N}{r_0 + h} ds . \quad (8)$$

To an accuracy of 1 percent,  $r_0 / (r_0 + h) \approx 1$ , so that Equation 8 simplifies to

$$b = - d \cos \gamma_0 \int N ds \quad (9)$$

where the integral extends from a point on the earth's surface to a point above the troposphere. By substituting the value of  $\int N ds$  from Equation 4 into Equation 9,

$$b = - \cot \gamma_0 N_s G(g) , \quad (10)$$

where

$$G(g) = \sqrt{\pi} g e^{g^2} (1 - \operatorname{erf} g), \quad (11)$$

$g$  having been defined by Equation 5.

## DETERMINATION OF THE PARAMETER $d$

The remaining problem is to determine the parameter  $d$  which occurs in the expression for the tropospheric contribution to the range  $\Delta R$ , which will be abbreviated TRA, "Tropospheric Range Adjustment."

For a target at 90 degrees elevation, from Equation 6

$$\text{TRA}_{90^\circ} = 10^{-6} \int_0^\infty N(h) dh = 10^{-6} \frac{N_s}{d}, \quad (12)$$

so that if  $\int_0^\infty N(h) dh$  is known, then  $d$  is fixed. For a given station, the fractional variation in  $\int_0^\infty N(h) dh$  is one half to one fourth as great as the fractional variation in  $N_s$ . Accordingly, as a first approximation, we may compute  $\overline{\text{TRA}}_{90^\circ}$ , the mean value of  $10^{-6} \int_0^\infty N(h) dh$  averaged over many profiles for a given site, considering it as a site constant (Reference 8). The parameter  $d$  is then determined from

$$d = 10^{-6} \frac{N_s}{\overline{\text{TRA}}_{90^\circ}} \quad (13)$$

The accuracy of this procedure, which for brevity will be designated "Method I," was tested against a set of 77 refractive index profiles furnished by the Boulder Laboratories of the National Bureau of Standards. These refractive index profiles were determined from radiosonde measurements taken at thirteen different weather stations covering a wide range of geographical conditions. Six types of profiles for each station (except one) were chosen by the Boulder Laboratories in order to include an extreme variety of profile behavior. The profile types are described in Reference 9 and are plotted in Figure 3, as well as in Figure 41 of Reference 10 which describes a different method of attack on the problem of range compensation. Each ray-tracing gave  $N(h)$ , slant range, the difference angle  $\epsilon = \theta_0 - \beta_0$ , and TRA as a function of target height for various initial elevation angles from 0 to 1.500 radians.

The values of the ray-traced  $\text{TRA}_{90^\circ}$  in meters for each profile of the thirteen different stations (at a height above 160 km) are entered in the column 12 of Table I, under the subheading "Method I" which designates the procedure of averaging the  $\text{TRA}_{90^\circ}$  to determine the site constant  $\overline{\text{TRA}}_{90^\circ}$ . The predicted values of  $\text{TRA}_{90^\circ}$  are entered in the column 11, and the rms prediction error in meters for each station is entered immediately below.

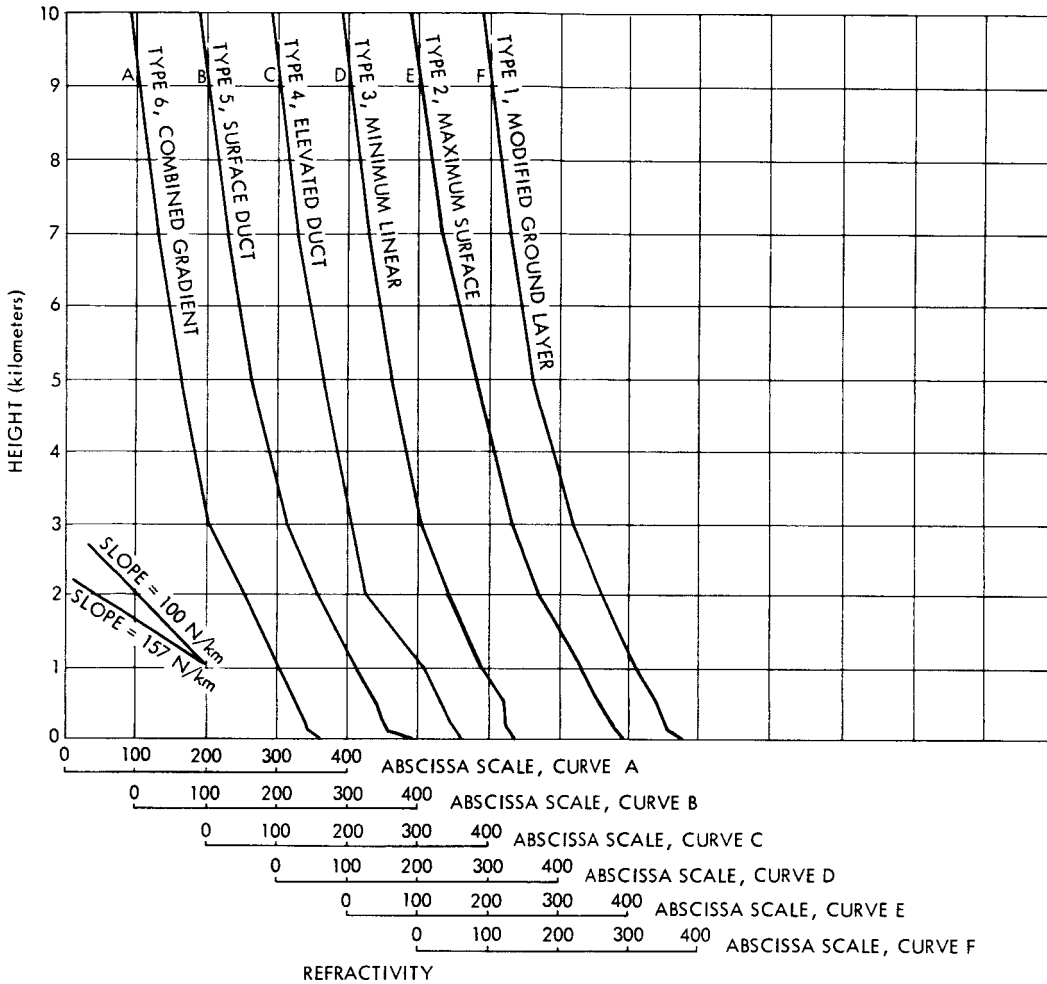


Figure 3—Refractivity vs. height for 6 profile types taken at Station 12839. (Note that a super-refractive profile is one containing a gradient 100 N-units per km but less than 157 N-units per km. A ducting profile is one containing a gradient exceeding 157 N-units per km.)

A second method, designated "Method II," for finding  $TRA_{90^\circ}$ , (and hence determining  $d$  from Equation 12) assumes a linear relationship between  $TRA_{90^\circ}$  and  $N_s$ .

By assuming

$$TRA_{90^\circ, p} = A + BN_s, \quad (14)$$

the values of  $A$  and  $B$  were determined for each station, by the method of least squares, from the measured values of  $TRA_{90^\circ}$  and  $N_s$  available from the 5 profile types enumerated in Table I. The values of  $TRA_{90^\circ, p}$ , the predicted value of  $TRA_{90^\circ}$ , are tabulated in the column 11 of Table I under the subheading "Method II" for each of the thirteen stations analyzed.

Table I

Predicted and Measured TRA Values. (The measured TRA values tabulated under "Meas." were obtained from the Boulder Laboratories, National Bureau of Standards, who ray-traced the refractivity profiles measured by radiosondes at the thirteen sites.)

## STATION 14764

## Method I

Profile	$N_s$	TRA for $\theta_0 = 20$ mr		TRA for $\theta_0 = 50$ mr		TRA for $\theta_0 = 100$ mr		TRA for $\theta_0 = 200$ mr		TRA for $\theta_0 = 90^\circ$	
		Pred.	Meas.	Pred.	Meas.	Pred.	Meas.	Pred.	Meas.	Pred.	Meas.
1	357.5	69.83	69.92	40.51	40.63	23.08	23.30	12.09	12.33	2.46	2.50
3	315.0	65.36	64.34	39.27	38.31	22.76	22.07	12.05	11.70	2.46	2.37
4	345.0	68.51	69.63	40.16	41.03	23.01	23.60	12.08	12.50	2.46	2.53
5	347.5	68.78	67.56	40.24	39.38	23.01	22.62	12.08	11.98	2.46	2.43
6	342.0	68.19		40.08	40.00	22.96	23.02	12.08	12.19	2.46	2.47
rms		0.87		0.69		0.45		0.28		0.06	

$$\text{Method II } \text{TRA}_{90^\circ, p} = 0.0029988 N_s + 1.4378$$

Profile	$N_s$	TRA for $\theta_0 = 20$ mr		TRA for $\theta_0 = 50$ mr		TRA for $\theta_0 = 100$ mr		TRA for $\theta_0 = 200$ mr		TRA for $\theta_0 = 90^\circ$	
		Pred.	Meas.	Pred.	Meas.	Pred.	Meas.	Pred.	Meas.	Pred.	Meas.
1	357.5	70.61	69.92	41.16	40.63	23.57	23.30	12.33	12.33	2.51	2.50
3	315.0	64.08	64.34	38.25	38.31	21.82	22.07	11.66	11.70	2.38	2.37
4	345.0	68.69	69.63	40.35	41.03	23.10	23.60	12.13	12.50	2.47	2.53
5	347.5	69.08	67.56	40.48	39.38	23.12	22.62	12.17	11.98	2.48	2.43
6	342.0	68.22		40.11	40.00	22.96	23.02	12.09	12.19	2.46	2.47
rms		0.88		0.63		0.36		0.19		0.04	

## STATION 13983

## Method I

Profile	$N_s$	TRA for $\theta_0 = 20$ mr		TRA for $\theta_0 = 50$ mr		TRA for $\theta_0 = 100$ mr		TRA for $\theta_0 = 200$ mr		TRA for $\theta_0 = 90^\circ$	
		Pred.	Meas.	Pred.	Meas.	Pred.	Meas.	Pred.	Meas.	Pred.	Meas.
1	367.0	69.46	71.08	40.21	40.96	22.75	23.37	11.89	12.35	2.42	2.50
3	309.5	64.09	63.27	38.55	37.74	22.37	21.76	11.84	11.53	2.42	2.34
4	307.5	63.89	62.24	38.51	37.16	22.36	21.49	11.84	11.41	2.42	2.32
5	365.0	69.89	70.88	40.15	40.97	22.74	23.47	11.89	12.42	2.42	2.52
6	346.0	67.90	67.07	40.18	39.13	22.62	22.50	11.87	11.93	2.42	2.42
rms		1.24		0.98		0.64		0.40		0.08	

$$\text{Method II } \text{TRA}_{90^\circ, p} = 0.0031294 N_s + 1.3579$$

Profile	$N_s$	TRA for $\theta_0 = 20$ mr		TRA for $\theta_0 = 50$ mr		TRA for $\theta_0 = 100$ mr		TRA for $\theta_0 = 200$ mr		TRA for $\theta_0 = 90^\circ$	
		Pred.	Meas.	Pred.	Meas.	Pred.	Meas.	Pred.	Meas.	Pred.	Meas.
1	367.0	71.60	71.08	41.38	40.96	23.52	23.37	12.32	12.35	2.51	2.50
3	309.5	62.74	63.27	37.47	37.74	21.66	21.76	11.39	11.53	2.33	2.34
4	307.5	62.30	62.24	37.22	37.16	21.52	21.49	11.36	11.41	2.32	2.32
5	365.0	71.29	70.88	41.24	40.97	23.45	23.47	12.29	12.42	2.50	2.52
6	346.0	68.27	67.07	39.92	39.13	22.81	22.50	11.98	11.93	2.44	2.42
rms		0.65		0.43		0.16		0.09		0.04	

Table I (continued)

Predicted and Measured TRA Values. (The measured TRA values tabulated under "Meas." were obtained from the Boulder Laboratories, National Bureau of Standards, who ray-traced the refractivity profiles measured by radiosondes at the thirteen sites.)

## STATION 12839

## Method I

Profile	$N_s$	TRA for $\theta_0 = 20$ mr		TRA for $\theta_0 = 50$ mr		TRA for $\theta_0 = 100$ mr		TRA for $\theta_0 = 200$ mr		TRA for $\theta_0 = 90^\circ$	
		Pred.	Meas.	Pred.	Meas.	Pred.	Meas.	Pred.	Meas.	Pred.	Meas.
1	376.5	72.96	73.29	41.92	42.20	23.75	24.12	12.42	12.76	2.53	2.59
3	333.6	68.37	67.62	40.67	40.09	23.47	23.13	12.38	12.28	2.53	2.49
4	360.0	71.18	70.14	41.45	40.78	23.64	23.40	12.40	12.40	2.53	2.52
5	379.5	73.29	72.52	42.01	41.43	23.77	23.60	12.42	12.46	2.53	2.52
6	358.5	71.02	70.14	41.40	40.79	23.63	23.40	12.40	12.39	2.53	2.51
rms		0.78		0.56		0.28		0.16		0.03	

$$\text{Method II } \text{TRA}_{90^\circ, p} = 0.0014149 N_s + 2.0148$$

Profile	$N_s$	TRA for $\theta_0 = 20$ mr		TRA for $\theta_0 = 50$ mr		TRA for $\theta_0 = 100$ mr		TRA for $\theta_0 = 200$ mr		TRA for $\theta_0 = 90^\circ$	
		Pred.	Meas.	Pred.	Meas.	Pred.	Meas.	Pred.	Meas.	Pred.	Meas.
1	376.5	73.32	73.29	42.20	42.20	23.93	24.12	12.52	12.76	2.55	2.59
3	333.6	67.74	67.62	40.16	40.09	23.13	23.13	12.19	12.28	2.49	2.49
4	360.0	71.15	70.14	41.42	40.78	23.62	23.40	12.40	12.40	2.52	2.52
5	379.5	73.72	72.52	42.35	41.43	23.99	23.60	12.54	12.46	2.55	2.52
6	358.5	70.95	70.14	41.35	40.79	23.60	23.40	12.38	12.39	2.52	2.51
rms		0.79		0.56		0.23		0.12		0.02	

## STATION 13742

## Method I

Profile	$N_s$	TRA for $\theta_0 = 20$ mr		TRA for $\theta_0 = 50$ mr		TRA for $\theta_0 = 100$ mr		TRA for $\theta_0 = 200$ mr		TRA for $\theta_0 = 90^\circ$	
		Pred.	Meas.	Pred.	Meas.	Pred.	Meas.	Pred.	Meas.	Pred.	Meas.
1	344.0	68.67	69.28	40.06	40.75	22.95	23.40	12.13	12.38	2.46	2.51
3	297.5	63.45	62.32	38.67	37.53	22.61	21.70	12.08	11.51	2.46	2.34
4	350.0	68.96	69.28	40.26	40.52	22.98	23.27	12.14	12.32	2.46	2.50
5	336.0	67.50	65.85	39.85	38.71	22.89	22.32	12.12	11.84	2.46	2.40
6	370.5	71.15	72.14	40.83	41.60	23.12	23.75	12.15	12.55	2.46	2.54
rms		1.05		0.86		0.72		0.35		0.08	

$$\text{Method II } \text{TRA}_{90^\circ, p} = 0.0030024 N_s + 1.4379$$

Profile	$N_s$	TRA for $\theta_0 = 20$ mr		TRA for $\theta_0 = 50$ mr		TRA for $\theta_0 = 100$ mr		TRA for $\theta_0 = 200$ mr		TRA for $\theta_0 = 90^\circ$	
		Pred.	Meas.	Pred.	Meas.	Pred.	Meas.	Pred.	Meas.	Pred.	Meas.
1	344.0	68.55	69.28	40.25	40.75	23.06	23.40	12.20	12.38	2.47	2.51
3	297.5	61.45	62.32	37.07	37.53	21.54	21.70	11.46	11.51	2.33	2.34
4	350.0	69.49	69.28	40.67	40.52	23.25	23.27	12.30	12.32	2.49	2.50
5	336.0	67.31	65.85	39.71	38.71	22.80	22.32	12.07	11.84	2.45	2.40
6	370.5	72.72	72.14	42.07	41.60	23.92	23.75	12.62	12.55	2.55	2.54
rms		0.87		0.58		0.28		0.13		0.03	

Table I (continued)

Predicted and Measured TRA Values. (The measured TRA values tabulated under "Meas." were obtained from the Boulder Laboratories, National Bureau of Standards, who ray-traced the refractivity profiles measured by radiosondes at the thirteen sites.)

## STATION 12921

## Method I

Profile	$N_s$	TRA for $\theta_0 = 20$ mr		TRA for $\theta_0 = 50$ mr		TRA for $\theta_0 = 100$ mr		TRA for $\theta_0 = 200$ mr		TRA for $\theta_0 = 90^\circ$	
		Pred.	Meas.	Pred.	Meas.	Pred.	Meas.	Pred.	Meas.	Pred.	Meas.
1	366.0	70.68	70.81	40.71	40.83	23.09	23.31	12.08	12.31	2.46	2.49
3	301.5	63.87	62.47	38.78	37.55	22.63	21.73	12.02	11.53	2.46	2.34
4	335.5	67.45	66.31	39.84	39.02	22.89	22.47	12.05	11.91	2.46	2.42
5	375.5	71.68	72.58	40.97	41.66	23.15	23.74	12.08	12.53	2.46	2.54
6	359.0	69.93	70.33	40.51	40.83	23.04	23.35	12.07	12.34	2.46	2.50
rms		0.92		0.75		0.55		0.34		0.07	

$$\text{Method II } \text{TRA}_{90^\circ, p} = 0.0026478 N_s + 1.5378$$

Profile	$N_s$	TRA for $\theta_0 = 20$ mr		TRA for $\theta_0 = 50$ mr		TRA for $\theta_0 = 100$ mr		TRA for $\theta_0 = 200$ mr		TRA for $\theta_0 = 90^\circ$	
		Pred.	Meas.	Pred.	Meas.	Pred.	Meas.	Pred.	Meas.	Pred.	Meas.
1	366.0	71.50	70.81	41.37	40.83	23.51	23.31	12.32	12.31	2.51	2.49
3	301.5	61.94	62.47	37.25	37.55	21.64	21.73	11.43	11.53	2.34	2.34
4	335.5	66.93	66.31	39.42	39.02	22.62	22.47	11.90	11.91	2.43	2.42
5	375.5	72.95	72.58	41.97	41.66	23.79	23.74	12.45	12.53	2.53	2.54
6	359.0	70.44	70.33	40.92	40.83	23.31	23.35	12.22	12.34	2.49	2.50
rms		0.51		0.36		0.13		0.08		0.01	

## STATION 23236

## Method I

Profile	$N_s$	TRA for $\theta_0 = 20$ mr		TRA for $\theta_0 = 50$ mr		TRA for $\theta_0 = 100$ mr		TRA for $\theta_0 = 200$ mr		TRA for $\theta_0 = 90^\circ$	
		Pred.	Meas.	Pred.	Meas.	Pred.	Meas.	Pred.	Meas.	Pred.	Meas.
1	340.0	68.72	69.66	40.60	41.22	23.34	23.69	12.29	12.54	2.51	2.54
3	323.5	66.97	65.87	40.10	39.14	23.22	22.55	12.28	11.95	2.51	2.42
4	339.5	68.66	69.24	40.58	41.38	23.33	24.19	12.29	12.94	2.51	2.64
5	337.0	68.45	69.61	40.51	41.31	23.32	23.77	12.29	12.58	2.51	2.55
6	330.0	67.66	64.74	40.30	38.19	23.27	22.06	12.28	11.71	2.51	2.38
rms		1.57		1.19		0.77		0.45		0.09	

$$\text{Method II } \text{TRA}_{90^\circ, p} = 0.0121697 N_s - 1.5582$$

Profile	$N_s$	TRA for $\theta_0 = 20$ mr		TRA for $\theta_0 = 50$ mr		TRA for $\theta_0 = 100$ mr		TRA for $\theta_0 = 200$ mr		TRA for $\theta_0 = 90^\circ$	
		Pred.	Meas.	Pred.	Meas.	Pred.	Meas.	Pred.	Meas.	Pred.	Meas.
1	340.0	69.90	69.66	41.55	41.22	23.96	23.69	12.65	12.54	2.58	2.54
3	323.5	65.48	65.87	38.91	39.14	22.43	22.55	11.82	11.95	2.38	2.42
4	339.5	69.77	69.24	41.47	41.38	23.91	24.19	12.62	12.94	2.57	2.64
5	337.0	68.99	69.61	40.98	41.31	23.63	23.77	12.47	12.58	2.54	2.55
6	330.0	66.87	64.74	39.67	38.19	22.85	22.06	12.04	11.71	2.46	2.38
rms		1.04		0.70		0.40		0.23		0.05	

Table I (continued)

Predicted and Measured TRA Values. (The measured TRA values tabulated under "Meas." were obtained from the Boulder Laboratories, National Bureau of Standards, who ray-traced the refractivity profiles measured by radiosondes at the thirteen sites.)

## STATION 23154

## Method I

Profile	$N_s$	TRA for $\theta_0 = 20$ mr Pred. Meas.		TRA for $\theta_0 = 50$ mr Pred. Meas.		TRA for $\theta_0 = 100$ mr Pred. Meas.		TRA for $\theta_0 = 200$ mr Pred. Meas.		TRA for $\theta_0 = 90^\circ$ Pred. Meas.	
1	280.0	53.58	54.97	31.70	32.84	18.39	19.00	9.69	10.09	1.96	2.05
3	249.5	50.72	49.72	20.86	29.98	18.02	17.36	9.66	9.22	1.96	1.87
4	255.0	51.24	51.06	31.02	30.84	18.06	17.90	9.67	9.51	1.96	1.93
5	267.0	52.36	52.35	31.35	31.45	18.14	18.24	9.68	9.69	1.96	1.97
rms		0.90		0.73		0.46		0.31		0.06	

$$\text{Method II } \text{TRA}_{90^\circ, p} = 0.0053940 N_s + 0.5421$$

Profile	$N_s$	TRA for $\theta_0 = 20$ mr Pred. Meas.		TRA for $\theta_0 = 50$ mr Pred. Meas.		TRA for $\theta_0 = 100$ mr Pred. Meas.		TRA for $\theta_0 = 200$ mr Pred. Meas.		TRA for $\theta_0 = 90^\circ$ Pred. Meas.	
1	280.0	55.20	54.97	32.98	32.84	19.05	19.00	10.17	10.09	2.05	2.05
3	249.5	49.63	49.72	30.01	29.98	17.45	17.36	9.33	9.22	1.89	1.87
4	255.0	50.63	51.06	30.70	30.84	17.74	17.90	9.48	9.51	1.92	1.93
5	267.0	52.81	52.35	31.71	31.45	18.37	18.24	9.82	9.69	1.98	1.97
rms		0.34		0.16		0.11		0.09		0.01	

## STATION 23062

## Method I

Profile	$N_s$	TRA for $\theta_0 = 20$ mr Pred. Meas.		TRA for $\theta_0 = 50$ mr Pred. Meas.		TRA for $\theta_0 = 100$ mr Pred. Meas.		TRA for $\theta_0 = 200$ mr Pred. Meas.		TRA for $\theta_0 = 90^\circ$ Pred. Meas.	
1	266.0	52.74	52.56	31.69	31.59	18.38	18.31	9.72	9.72	1.98	1.97
3	237.0	49.97	50.54	30.85	31.07	18.16	18.14	9.69	9.65	1.98	1.96
4	278.0	53.87	53.04	32.02	31.56	18.45	18.24	9.73	9.67	1.98	1.96
5	254.0	51.60	50.99	31.35	30.97	17.79	18.07	9.71	9.63	1.98	1.96
6	286.0	54.62	55.16	32.23	32.88	18.52	19.07	9.74	10.14	1.98	2.06
rms		0.58		0.41		0.29		0.19		0.04	

$$\text{Method II } \text{TRA}_{90^\circ, p} = 0.0014731 N_s + 1.5942$$

Profile	$N_s$	TRA for $\theta_0 = 20$ mr Pred. Meas.		TRA for $\theta_0 = 50$ mr Pred. Meas.		TRA for $\theta_0 = 100$ mr Pred. Meas.		TRA for $\theta_0 = 200$ mr Pred. Meas.		TRA for $\theta_0 = 90^\circ$ Pred. Meas.	
1	266.0	52.38	52.56	31.73	31.59	18.42	18.31	9.74	9.72	1.99	1.97
3	237.0	49.34	50.54	30.35	31.07	17.83	18.14	9.50	9.65	1.94	1.96
4	278.0	54.21	53.04	32.29	31.56	18.64	18.24	9.83	9.67	2.00	1.96
5	254.0	51.35	50.99	31.16	30.97	18.19	18.07	9.64	9.63	1.97	1.96
6	286.0	55.16	55.16	32.65	32.88	18.79	19.07	9.90	10.14	2.02	2.06
rms		0.77		0.48		0.27		0.15		0.03	

Table I (continued)

Predicted and Measured TRA Values. (The measured TRA values tabulated under "Meas." were obtained from the Boulder Laboratories, National Bureau of Standards, who ray-traced the refractivity profiles measured by radiosondes at the thirteen sites.)

## STATION 24011

## Method I

Profile	$N_s$	TRA for $\theta_0 = 20$ mr		TRA for $\theta_0 = 50$ mr		TRA for $\theta_0 = 100$ mr		TRA for $\theta_0 = 200$ mr		TRA for $\theta_0 = 90^\circ$	
		Pred.	Meas.	Pred.	Meas.	Pred.	Meas.	Pred.	Meas.	Pred.	Meas.
1	322.5	63.60	62.99	37.48	37.05	21.51	21.31	11.32	11.28	2.31	2.29
3	295.0	60.80	59.45	36.68	35.51	21.32	20.48	11.29	10.86	2.31	2.20
4	314.5	62.79	64.40	37.25	38.40	21.45	22.14	11.31	11.73	2.31	2.38
5	341.5	65.54	65.46	38.01	38.09	21.63	21.90	11.33	11.60	2.31	2.35
6	318.0	63.14	62.99	37.35	37.27	21.48	21.49	11.31	11.40	2.31	2.31
rms		0.98		0.76		0.51		0.30		0.06	

$$\text{Method II } \text{TRA}_{90^\circ, P} = 0.0028108 N_s + 1.41257$$

Profile	$N_s$	TRA for $\theta_0 = 20$ mr		TRA for $\theta_0 = 50$ mr		TRA for $\theta_0 = 100$ mr		TRA for $\theta_0 = 200$ mr		TRA for $\theta_0 = 90^\circ$	
		Pred.	Meas.	Pred.	Meas.	Pred.	Meas.	Pred.	Meas.	Pred.	Meas.
1	322.5	63.81	62.99	37.64	37.05	21.61	21.31	11.38	11.28	2.32	2.29
3	295.0	59.77	59.45	35.85	35.51	20.77	20.48	10.98	10.86	2.24	2.20
4	314.5	62.69	64.40	37.17	38.40	21.40	22.14	11.28	11.73	2.30	2.38
5	341.5	66.66	65.46	38.89	38.09	22.20	21.90	11.66	11.60	2.37	2.35
6	318.0	63.17	62.99	37.35	37.27	21.48	21.49	11.31	11.41	2.31	2.31
rms		1.02		0.73		0.40		0.25		0.04	

## STATION 14834

## Method I

Profile	$N_s$	TRA for $\theta_0 = 20$ mr		TRA for $\theta_0 = 50$ mr		TRA for $\theta_0 = 100$ mr		TRA for $\theta_0 = 200$ mr		TRA for $\theta_0 = 90^\circ$	
		Pred.	Meas.	Pred.	Meas.	Pred.	Meas.	Pred.	Meas.	Pred.	Meas.
1	390.5	73.64	74.10	40.99	41.95	23.10	23.81	11.96	12.55	2.43	2.54
3	309.5	64.26	63.75	38.68	38.12	22.46	22.00	11.89	11.67	2.43	2.37
4	320.0	65.37	65.30	39.01	38.88	22.54	22.43	11.90	11.89	2.43	2.41
5	337.0	67.15	66.61	39.51	39.09	22.66	22.46	11.92	11.89	2.43	2.41
6	340.0	67.45	66.47	39.59	38.97	22.67	22.44	11.92	11.90	2.43	2.41
rms		0.59		0.60		0.41		0.29		0.06	

$$\text{Method II } \text{TRA}_{90^\circ, P} = 0.0020427 N_s + 1.7359$$

Profile	$N_s$	TRA for $\theta_0 = 20$ mr		TRA for $\theta_0 = 50$ mr		TRA for $\theta_0 = 100$ mr		TRA for $\theta_0 = 200$ mr		TRA for $\theta_0 = 90^\circ$	
		Pred.	Meas.	Pred.	Meas.	Pred.	Meas.	Pred.	Meas.	Pred.	Meas.
1	390.5	73.84	74.10	42.41	41.95	23.90	23.81	12.47	12.55	2.53	2.54
3	309.5	62.83	63.75	37.90	38.12	21.94	22.00	11.59	11.67	2.37	2.37
4	320.0	64.23	65.30	38.49	38.88	22.18	22.43	11.71	11.89	2.39	2.41
5	337.0	67.05	66.61	39.45	39.09	22.61	22.46	11.92	11.89	2.42	2.41
6	340.0	67.46	66.47	39.61	38.97	22.68	22.44	11.93	11.90	2.43	2.41
rms		0.80		0.44		0.18		0.10		0.01	

Table I (continued)

Predicted and Measured TRA Values. (The measured TRA values tabulated under "Meas." were obtained from the Boulder Laboratories, National Bureau of Standards, who ray-traced the refractivity profiles measured by radiosondes at the thirteen sites.)

## STATION 24240

## Method I

Profile	$N_s$	TRA for $\theta_0 = 20$ mr		TRA for $\theta_0 = 50$ mr		TRA for $\theta_0 = 100$ mr		TRA for $\theta_0 = 200$ mr		TRA for $\theta_0 = 90^\circ$	
		Pred.	Meas.	Pred.	Meas.	Pred.	Meas.	Pred.	Meas.	Pred.	Meas.
1	336.5	66.32	66.43	38.89	39.07	22.26	22.49	11.80	11.92	2.38	2.42
3	315.0	64.10	63.86	38.26	37.93	22.11	21.82	11.79	11.55	2.38	2.34
4	326.0	65.24	65.07	38.80	38.49	22.19	22.17	11.80	11.75	2.38	2.38
5	337.0	66.37	66.05	38.90	38.85	22.26	22.45	11.81	11.92	2.38	2.42
6	323.0	64.93	64.31	38.50	38.04	22.17	21.91	11.79	11.61	2.38	2.36
rms		0.34		0.30		0.22		0.15		0.03	

Method II  $\text{TRA}_{90^\circ, p} = 0.0037050 N_s + 1.16999$ 

Profile	$N_s$	TRA for $\theta_0 = 20$ mr		TRA for $\theta_0 = 50$ mr		TRA for $\theta_0 = 100$ mr		TRA for $\theta_0 = 200$ mr		TRA for $\theta_0 = 90^\circ$	
		Pred.	Meas.	Pred.	Meas.	Pred.	Meas.	Pred.	Meas.	Pred.	Meas.
1	336.5	66.87	66.43	39.33	39.07	22.55	22.49	11.97	11.92	2.42	2.42
3	315.0	63.34	63.86	37.67	37.93	21.72	21.82	11.56	11.55	2.34	2.34
4	326.0	65.14	65.07	38.51	38.49	22.14	22.17	11.77	11.75	2.38	2.38
5	337.0	66.96	66.05	39.36	38.85	22.56	22.45	11.98	11.92	2.42	2.42
6	323.0	64.65	64.31	38.28	38.04	22.03	21.91	11.71	11.61	2.37	2.36
rms		0.53		0.30		0.09		0.06		0.01	

## STATION 99999

## Method I

Profile	$N_s$	TRA for $\theta_0 = 20$ mr		TRA for $\theta_0 = 50$ mr		TRA for $\theta_0 = 100$ mr		TRA for $\theta_0 = 200$ mr		TRA for $\theta_0 = 90^\circ$	
		Pred.	Meas.	Pred.	Meas.	Pred.	Meas.	Pred.	Meas.	Pred.	Meas.
1	388.5	75.71	76.27	43.40	43.71	24.56	24.85	12.83	12.10	2.61	2.65
3	383.5	75.16	75.67	43.26	43.56	24.53	24.81	12.83	13.09	2.61	2.65
4	373.5	74.06	71.66	42.97	41.12	24.58	23.46	12.82	12.39	2.61	2.51
5	402.5	77.27	76.89	43.80	43.35	24.65	24.55	12.84	12.93	2.61	2.62
6	393.5	76.27	76.15	43.54	43.35	24.59	24.62	12.84	12.98	2.61	2.63
rms		1.14		0.87		0.54		0.27		0.05	

Method II  $\text{TRA}_{90^\circ, p} = 0.0031263 N_s + 1.3974$ 

Profile	$N_s$	TRA for $\theta_0 = 20$ mr		TRA for $\theta_0 = 50$ mr		TRA for $\theta_0 = 100$ mr		TRA for $\theta_0 = 200$ mr		TRA for $\theta_0 = 90^\circ$	
		Pred.	Meas.	Pred.	Meas.	Pred.	Meas.	Pred.	Meas.	Pred.	Meas.
1	388.5	75.72	76.27	43.42	43.71	24.57	24.85	12.83	13.10	2.61	2.65
3	383.5	74.91	75.67	43.06	43.56	24.40	24.81	12.75	13.09	2.60	2.65
4	373.5	73.29	71.66	42.35	41.12	24.07	23.46	12.59	12.39	2.57	2.51
5	402.5	78.02	76.89	44.40	43.35	25.04	24.55	13.06	12.93	2.66	2.62
6	393.5	76.54	76.15	43.77	43.35	24.73	24.62	12.92	12.98	2.63	2.63
rms		0.99		0.79		0.42		0.22		0.04	

Table I (continued)

Predicted and Measured TRA Values. (The measured TRA values tabulated under "Meas." were obtained from the Boulder Laboratories, National Bureau of Standards, who ray-traced the refractivity profiles measured by radiosondes at the thirteen sites.)

STATION 26411

## Method I

Profile	$N_s$	TRA for $\theta_0 = 20$ mr		TRA for $\theta_0 = 50$ mr		TRA for $\theta_0 = 100$ mr		TRA for $\theta_0 = 200$ mr		TRA for $\theta_0 = 90^\circ$	
		Pred.	Meas.	Pred.	Meas.	Pred.	Meas.	Pred.	Meas.	Pred.	Meas.
1	313.1	63.41	62.99	37.81	37.41	21.83	21.53	11.53	11.41	2.35	2.31
3	291.0	61.12	60.84	37.13	36.69	21.67	21.23	11.51	11.26	2.35	2.28
4	328.0	64.92	65.45	38.24	38.66	21.93	22.26	11.54	11.79	2.35	2.39
5	305.0	62.56	63.48	37.56	38.13	21.77	22.04	11.52	11.69	2.35	2.37
6	307.0	62.77	63.96	37.62	38.46	21.79	22.27	11.52	11.83	2.35	2.40
rms		0.75		0.56		0.37		0.23		0.05	

Method II  $\overline{\text{TRA}}_{90^\circ, p} = 0.0022295 N_s + 1.6635$ 

Profile	$N_s$	TRA for $\theta_0 = 20$ mr		TRA for $\theta_0 = 50$ mr		TRA for $\theta_0 = 100$ mr		TRA for $\theta_0 = 200$ mr		TRA for $\theta_0 = 90^\circ$	
		Pred.	Meas.	Pred.	Meas.	Pred.	Meas.	Pred.	Meas.	Pred.	Meas.
1	313.1	63.55	62.99	37.92	37.41	21.91	21.53	11.58	11.41	2.36	2.31
3	291.0	60.50	60.84	36.63	36.69	21.34	21.23	11.31	11.26	2.31	2.28
4	328.0	65.63	65.45	38.79	38.66	22.30	22.26	11.75	11.79	2.39	2.39
5	305.0	62.42	63.48	37.51	38.13	21.70	22.04	11.48	11.69	2.34	2.37
6	307.0	62.70	63.96	37.57	38.46	21.75	22.27	11.50	11.83	2.35	2.40
rms		0.80		0.54		0.33		0.19		0.04	

## THE COMPUTATION PROCEDURE

For each profile, then,  $\text{TRA}_{90^\circ}$  is estimated either by using Method I ( $\overline{\text{TRA}}_{90^\circ}$ ) or Method II ( $\text{TRA}_{90^\circ, p}$ ). The parameter  $d$  is determined by dividing  $N_s$  by this estimate as in Equation 12. As mentioned, substituting the above parameters, together with the angle  $\theta_0$ , into Equation 4 for  $\Delta R$  yields too small a correction and a two-step iterated computation becomes necessary: (1) com-

puting the approximate bending angle  $b_0$ , by integrating the normal component of the gradient of refractivity along the apparent line of sight, i.e., by using Equation 10 with  $\gamma_0 = \theta_0$ , and (2) integrating the refractivity along the radial  $\gamma_0 = \theta_0 - 0.5 b_0$ , i.e., setting  $\alpha = 0.5$ . However, it was found that a negative bias of over 2 m in TRA prediction at  $1^\circ$  elevation still remained. Modifying step 2 by integrating along the radial  $\theta_0 - 0.75 b_0$  reduced the bias considerably, as shown in Table 2.

Table 2

Effect of  $\gamma_0$  on TRA Prediction Error for  
Station 12,839,  $\theta_0 = 20$  mr ( $\sim 1^\circ$ )

Profile	Predicted TRA (m) ( $\theta_0 - 0.50 b_0$ )	True TRA (m)	Error (m)	Predicted TRA (m) ( $\theta_0 - 0.75 b_0$ )	Error (m)
1	69.90	73.29	-3.39	72.96	-0.33
3	65.78	67.62	-1.84	68.37	+0.75
4	68.10	70.14	-2.04	71.18	+1.04
5	69.80	72.52	-2.72	73.29	+0.77
6	67.93	70.13	-2.20	71.02	+0.89

It appears that integrating the refractivity along some radial intermediate between  $\theta_0 - 0.5 b_0$  and  $\theta_0 - 0.75 b_0$  would give a still more accurate prediction of TRA. However, since the rms error in the prediction of TRA at  $\theta_0 = 20 \text{ mr}$  ( $\approx 1^\circ$ ) is roughly 1 m, and since this appears entirely acceptable, it was decided not to further refine the prediction procedure.

The computing procedure then consists of the following three steps:

1. Obtain  $N_s$ ,  $\theta_0$ , and the exponential factor  $d$ , in  $N = N_s e^{-d(h-h_s)}$ . The factor  $d$  may be determined either by Method I (constant equivalent tropospheric thickness) or Method II (regression analysis).
2. Compute the approximate bending angle  $b_0$ ,

$$b_0 = -\cot \theta_0 N_s G(g) , \quad (10)$$

where

$$G(g) = \sqrt{\pi} g e^{g^2} (1 - \text{erf } g) , \quad (11)$$

$$g = \sqrt{\frac{dr_0}{2}} \tan \theta_0 . \quad (5)$$

3. Let

$$\theta' = \theta_0 - \frac{3b_0}{4} \quad (15)$$

and compute

$$\text{TRA}_{\theta_0} = \frac{10^{-6} N_s}{d \sin \theta'} G(g') \quad (16)$$

where

$$g' = \sqrt{\frac{dr_0}{2}} \tan \theta' . \quad (17)$$

## PREDICTION RESULTS

Predictions of TRA were computed for the thirteen stations and 5 profile types indicated in Table I using Method I and Method II. The 6<sup>th</sup> profile type, number 2, was reserved for independent testing, to be explained below. Table I summarizes the results of these predictions for all thirteen stations, giving the predicted and measured TRA, as well as the rms error in meters, for

each station, for various initial ray elevations from 20 mr ( $\approx 1^\circ$ ) to  $90^\circ$ . The overall rms prediction errors of the 5 profiles for the different stations are in Table 3.

Table 3

Overall rms Prediction Error (meters).

Method	$\theta_0 = 20 \text{ mr}$ ( $\approx 1^\circ$ )	$\theta_0 = 50 \text{ mr}$ ( $\approx 3^\circ$ )	$\theta_0 = 100 \text{ mr}$ ( $\approx 6^\circ$ )	$\theta_0 = 200 \text{ mr}$ ( $\approx 12^\circ$ )	$\theta_0 = 90^\circ$
I	0.95	0.75	0.50	0.30	0.062
II	0.80	0.54	0.28	0.16	0.032

Because only 5 samples of profiles were used to determine the station parameters, the predictions involve not merely knowledge of  $N_s$ , but, to some small degree, knowledge of  $\int N(h) dh$  for each profile. To eliminate this slight dependence on information regarding the profile whose TRA is being predicted, predictions were made for a type 2 profile using the site characteristics already computed from the other 5 profile types. The rms prediction errors averaged over all the stations are tabulated in Table 4 for initial ray angles of 20 mr ( $\approx 1^\circ$ ), 50 mr ( $\approx 3^\circ$ ), 100 mr ( $\approx 6^\circ$ ), and 200 mr ( $\approx 12^\circ$ ).

Table 4

Prediction Errors in rms for Type 2 Profiles (meters).

Method	$\theta_0 = 20 \text{ mr}$ ( $\approx 1^\circ$ )	$\theta_0 = 50 \text{ mr}$ ( $\approx 3^\circ$ )	$\theta_0 = 100 \text{ mr}$ ( $\approx 6^\circ$ )	$\theta_0 = 200 \text{ mr}$ ( $\approx 12^\circ$ )
I	1.63	1.23	0.89	0.57
II	0.82	0.65	0.42	0.27

The predicted TRA for this profile type had a negative bias, being almost always less than the measured value. This would appear to be due to the unusual nature of the profile, since by definition (Reference 9) it is the "profile with the highest value of  $N_s$  found for that station over period of record, but *not* having an initial gradient in excess of 100 N-units per km, nor any elevated layer with a gradient in

excess of 156.9 N-units per km." Nevertheless, the rms error for Method II is still less than 1 m at 1 degree target elevation.

On comparing the accuracy of the prediction methods described herein with that of the Convair method (Reference 10), it can be seen that the latter deteriorates rapidly at low angles, its residual error for  $\theta = 0.57^\circ$  exceeding 12 m (see Table 10, Reference 10); for the same angle, the residual error of a method described in Table 5, type 2 profiles (Method II), equals 1.67 m. It should be mentioned that the TRA data which were ray-traced by Convair, and which constitute the raw data from which their predictions are derived, differ considerably from the results computed by NBS, the difference arising partly from an approximation in the Convair ray-tracing program whose error becomes appreciable at low angles.

The samples in Table 5, taken at random, illustrate the magnitude of the differences in computed TRA. Besides the large discrepancies in  $\text{TRA}_{0^\circ}$ , even the  $\text{TRA}_{90^\circ}$  data differ by as much as 2 percent.

Because the NBS ray-tracing program has been carefully checked and analyzed for accuracy (Reference 3), the differences between the TRA computed by NBS and Convair are attributed to computational errors in the latter's program.

## CONCLUSION

This investigation has demonstrated that, in lieu of measuring the refractivity profile, ray-tracing the measured profile, and thereby determining the tropospheric range adjustment to be made for the indicated range, the tropospheric range adjustment may be approximated in realtime within a few percent by using a simple formula (Equation 16) into which the surface refractivity is substituted. Even for the extremely atypical profiles tested, the rms error in predicted TRA amounted to only 1.6 m at  $\theta_0 = 20$  mr ( $\approx 1^\circ$ ) target elevation for Method I, and half this amount for Method II. For less atypical profiles, the prediction errors will certainly be less, ranging roughly from about 1 m  $\theta_0 = 20$  mr ( $\approx 1^\circ$ ) to about 0.06 m at  $90^\circ$ .

## ACKNOWLEDGMENTS

It is a pleasure to acknowledge the continual advice and aid of Dr. F. O. Vonbun and Dr. R. Lehnert. Mr. B. R. Bean and Mr. G. D. Thayer of the Boulder Laboratories, National Bureau of Standards, made available the ray-tracings of the 77 profiles used for evaluating prediction procedures. Mr. Joseph Hilsenrath of the National Bureau of Standards, Washington, D. C., provided OMNITAB (Reference 11), a general interpretive machine program.

(Manuscript received October 29, 1963)

## REFERENCES

1. Guier, W. H., and Weiffenbach, G. C., "A Satellite Doppler Navigation System," *Proc. IRE* 48(4):507-516, April 1960.
2. Bean, B. R., and Thayer, G. D., "Models of the Atmospheric Radio Refractive Index," *Proc. IRE* 47(5):740-755, May 1959.
3. Bean, B. R., and Thayer, G. D., "CRPL Exponential Reference Atmosphere," Nat. Bur. Stand. Monogr. 4, Washington: U. S. Department of Commerce, National Bureau of Standards, 1959.
4. Hoehndorf, F. W., "Accuracy Limits Due to Refraction on Electronic Tracking of Space Vehicles," Air Force Off. Scientific Res. Technical Report 107, April 1961.

Table 5

Comparison Between Convair and NBS Computations of TRA.

Station	Profile type	TRA <sub>0°</sub> (m)		TRA <sub>90°</sub> (m)	
		Convair	NBS	Convair	NBS
14834	6	105.9	206.2	2.32	2.41
12839	4	109.7	130.5	2.57	2.52
13983	6	93.75	104.7	2.315	2.36
14764	4	108.19	126.27	2.565	2.53
23062	6	98.9	149.6	2.09	2.06
23236	6	107.23	142.3	2.422	2.376

5. Freeman, J. J., "Range-Error Compensation for a Troposphere with Exponentially Varying Refractivity," *J. Res. Nat. Bur. Stand.* 66D(6):695-697, November-December 1962.
6. Thayer, G. D., "A Formula for Radio Ray Refraction in an Exponential Atmosphere," *J. Res. Nat. Bur. Stand.* 65D(2):181-182, March-April 1961.
7. Chernov, L. A., "Wave Propagation in a Random Medium," (Translated from Russian by R. A. Silverman): New York: McGraw-Hill, 1960, Equation 24, p. 15.
8. Bauer, J. R., Mason, W. C., and Wilson, F. A., "Radio Refraction in a Cool Exponential Atmosphere," MIT Lincoln Laboratory, Lexington, Report LL-TR-186, August 27, 1958.
9. Bean, B. R., Cahoon, B. A., and Thayer, G. D., "Tables for the Statistical Prediction of Ray Bending and Elevation Angle Error Using Surface Values of the Refractive Index," Nat. Bur. Stand. Technical Note 44, March 16, 1960.
10. Rutledge, C. K., et al., "Precise Long Range Radar Distance Measuring Techniques," General Dynamics, Convair-Astronautics, San Diego, California, Report AE61-0061, February 13, 1961.
11. Hilsenrath, J., Zeigler, G. G., and Walsh, P. J., "OMNITAB: A General Purpose Machine Program for the Calculation of Tables and Functions and Statistical and Numerical Analysis of Tabular Data," Nat. Bur. Stand., to be published.